

Available online at www.sciencedirect.com

ScienceDirect

Advances in Space Research xxx (xxxx) xxx

ADVANCES IN SPACE RESEARCH (a COSPAR publication)

www.elsevier.com/locate/asr

The RAM-SCB model and its applications to advance space weather forecasting

V.K. Jordanova ^{a,*}, S.K. Morley ^a, M.A. Engel ^a, H.C. Godinez ^a, K. Yakymenko ^a M.G. Henderson ^a, Y. Yu ^b, Y. Miyoshi ^c

^a Los Alamos National Laboratory, PO Box 1663, MS B241, Los Alamos, NM 87545, USA
 ^b School of Space and Environment, Beihang University, Beijing 100191, China
 ^c Institute for Space-Earth Environmental Research, Nagoya University, Nagoya 464-8601, Japan

Received 4 March 2022; received in revised form 18 July 2022; accepted 28 August 2022

Abstract

Energetic particle fluxes that are part of the Earth's ring current and radiation belts can intensify significantly during space weather events like geomagnetic storms and could cause severe damage to satellite-based technologies. Understanding the physical processes that control their dynamics and improving our capability for their prediction is thus extremely important. In the context of space weather applications and user needs, this paper provides a brief description of our kinetic ring current-atmosphere interactions model with self-consistent magnetic field (RAM-SCB) and its further extension to implement a self-consistent electric (E) field. Specific examples that demonstrate RAM-SCB capabilities and limitations to reproduce the near-Earth space weather environment are given. The current status of RAM-SCB is assessed and plans for its further improvement are discussed.

© 2022 COSPAR. Published by Elsevier B.V. All rights reserved.

1. Introduction

The highly dynamic conditions in the near-Earth space environment, known as "space weather", affect a variety of sophisticated technologies our society is increasingly dependent on. Among the space-borne technologies are broadcast TV/Radio, cell phones, GPS, internet, commercial/military/scientific satellites, etc. Spacecraft users and operators need a good representation of this plasma environment since, for example, charged particles

can cause a buildup of charge on spacecraft materials and interfere with satellite functioning (Gubby and Evans, 2002). Ground-based technologies such as high voltage transmission lines and electric power grids are also affected by space weather events and specifically by the geomagnetically induced currents (GICs) due to variable magnetic fields at Earth's surface (Mate et al., 2021). Prediction of severe space weather events is highly desirable to allow for advanced preparation and protective actions (Morley, 2020). Therefore, the complex interactions that occur in the inner region of the magnetosphere, driven by processes on the Sun and modified by local conditions, are of much concern to space scientists and researchers. Large efforts to develop accurate models of this space plasma environment with both nowcasting and predictive capabilities are ongoing. This paper provides a brief description of the physics and numerical implementation of one such model

E-mail address: vania@lanl.gov (V.K. Jordanova).

https://doi.org/10.1016/j.asr.2022.08.077

0273-1177/ \circledcirc 2022 COSPAR. Published by Elsevier B.V. All rights reserved.

Abbreviations: RAM-SCB, Ring current – Atmosphere interactions Model with Self-Consistent magnetic (B) field; SHIELDS, Space Hazards Induced near Earth by Large Dynamic Storms; SWMF, Space Weather Modeling Framework

^{*} Corresponding author.

(RAM-SCB) that has grown from a research-grade code with limited options to a rich, highly configurable research and operations tool with a multitude of applications and output products.

observed particle flux data from geosynchronous (GEO) satellites or from other models.

2. Model description

The Ring current – Atmosphere interactions Model (RAM) with self-consistent (SC) magnetic (B) field is a unique code that combines a kinetic model of ring current plasma with a three-dimensional (3-D) force-balanced model of the terrestrial magnetic field. The two codes work in tandem, with RAM providing anisotropic pressure to SCB and SCB returning the self-consistently calculated magnetic field through which RAM plasma is advected; a schematic representation is shown in Fig. 1. The code has currently been expanded to include a self-consistent calculation of the electric (E) field too, and this version is abbreviated as RAM-SCB-E. The realistic inflow of plasma from the magnetotail during storm-time is specified from

2.1. Ring current – Atmosphere interactions model (RAM)

The Ring current-Atmosphere interactions Model (RAM) (Jordanova et al., 1996, 1997, 2008, 2010b) was developed to study the transport, acceleration and loss of ring current ions and relativistic electrons in near-Earth space. It differs from other ring current models that use adiabatic invariants as independent variables, by tracking the variables energy (E) and equatorial pitch angle (α_o), which makes direct comparison of model results with observations easier. It solves numerically the bounce-averaged kinetic equation for the phase space distribution function $Q_l(R_o, \phi, E, \mu_o, t)$ of species l as a function of time:

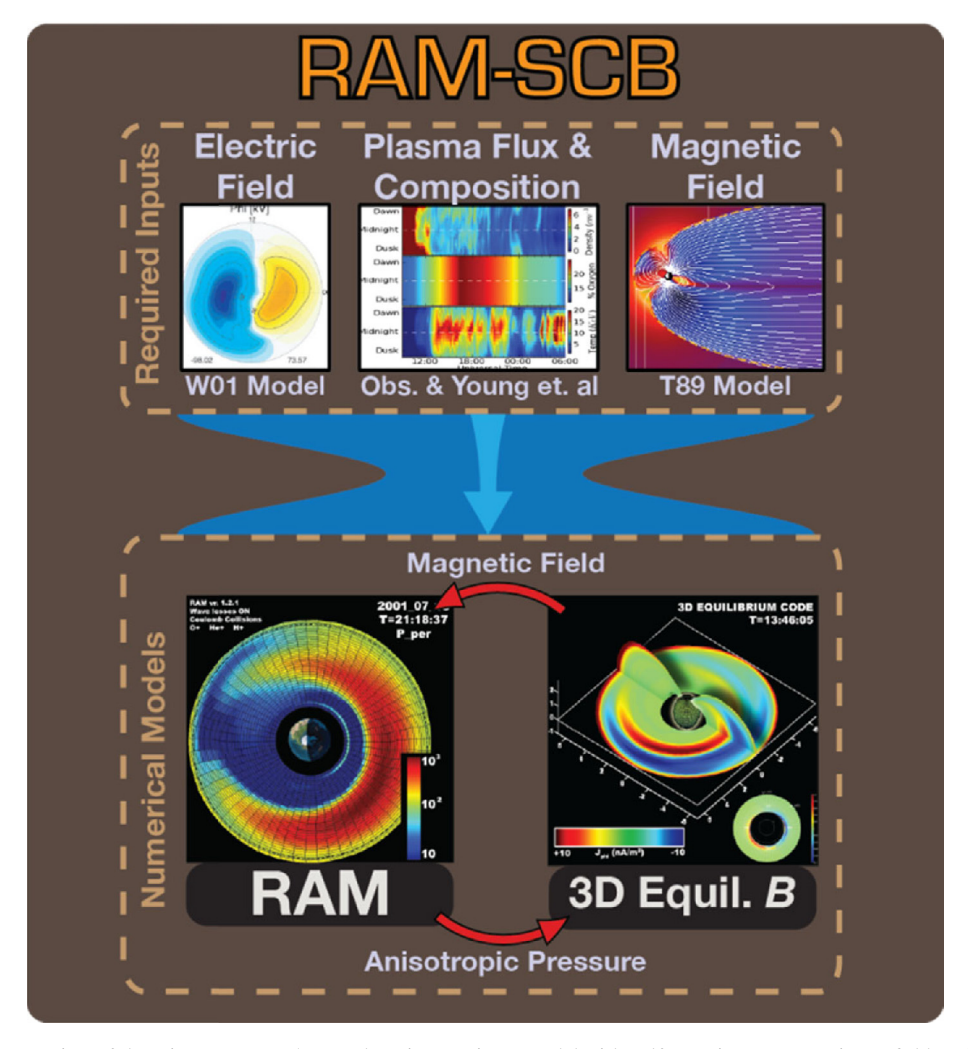


Fig. 1. Schematic representation of the Ring current – Atmosphere interactions Model with Self-Consistent magnetic (B) field (RAM-SCB). The model is driven by spatially- and temporally-varying electric and magnetic fields, obtained from empirical models (e.g., Weimer, 2001; Tsyganenko, 1989) or calculated self-consistently. The plasma boundary conditions are obtained from geosynchronous observations or from other models.

Please cite this article as: V. K. Jordanova, S. K. Morley, M. A. Engel et al., The RAM-SCB model and its applications to advance space weather forecasting, Advances in Space Research, https://doi.org/10.1016/j.asr.2022.08.077

$$\frac{\partial Q_{l}}{\partial t} + \frac{1}{R_{o}^{2}} \frac{\partial}{\partial R_{o}} \left(R_{o}^{2} \langle \frac{\mathrm{d}R_{o}}{\mathrm{d}t} \rangle Q_{l} \right) + \frac{\partial}{\partial \phi} \left(\langle \frac{d\phi}{\mathrm{d}t} \rangle Q_{l} \right) + \frac{1}{\gamma p} \frac{\partial}{\partial E} \left(\gamma p \langle \frac{\mathrm{d}E}{\mathrm{d}t} \rangle Q_{l} \right) + \frac{1}{h\mu_{o}} \frac{\partial}{\partial \mu_{o}} \left(h\mu_{o} \langle \frac{d\mu_{o}}{\mathrm{d}t} \rangle Q_{l} \right) = \left\langle \left(\frac{\partial Q_{l}}{\partial t} \right)_{\mathrm{cc}} \right\rangle + \left\langle \left(\frac{\partial Q_{l}}{\partial t} \right)_{\mathrm{cc}} \right\rangle + \left\langle \left(\frac{\partial Q_{l}}{\partial t} \right)_{\mathrm{sc}} \right\rangle + \left\langle \left(\frac{\partial Q_{l}}{\partial t} \right)_{\mathrm{atm}} \right\rangle \tag{1}$$

Here p is the relativistic momentum of the particle, γ is the relativistic factor, R_0 is the radial distance in the magnetic equatorial plane (from 2 to 6.5 R_E by default), ϕ is the geomagnetic east longitude (or magnetic local time, MLT), E is the kinetic energy of the particle (from ~ 0.1 to ~ 500 keV), α_o is the equatorial pitch angle (from 0° to 90°) and $\mu_o = \cos(\alpha_o)$. The index o refers to quantities in the magnetic equatorial plane and the brackets < > denote bounce averaging; this formalism is applicable in regions where the first two adiabatic invariants are conserved, which is typically true for the inner magnetosphere (Wolf, 1983). The purely field-geometric integral $h = 1/(2R_o) \int ds/\sqrt{(1-B(s)/B_m)}$ is calculated along the field lines and between the mirror points where the field intensity is B_m . At present the code includes four ion species (H⁺, He⁺, N⁺ and O⁺) and it is set up to easily accept new ion species.

The left-hand side of Eq. (1) describes the transport and acceleration of charged particles in time-dependent electric (convection and corotation) and magnetic fields. RAM can be easily updated to incorporate various electric and magnetic field models. At present, the choice of electric field models includes Volland-Stern (V-S) (Volland, 1973; Stern, 1975), Weimer (2001, 2005), and self-consistent (SCE) (Yu et al., 2017). The choice of magnetic field models includes dipole, Tsyganenko (1989, 1996), Tsyganenko and Sitnov (2005), and self-consistent (SCB) (Zaharia et al., 2006). The terms on the right-hand side represent different loss mechanisms; at present they include charge exchange, both energy and pitch angle scattering by Coulomb collisions, wave induced and field line curvature scattering, and loss to the atmosphere. Many of these losses depend on the cold plasma densities and to this end RAM is coupled with a time-dependent plasmasphere model (Rasmussen et al., 1993). The geocoronal hydrogen density model of Rairden et al. (1986) is used to calculate losses due to charge exchange. The ion and electron scattering by electro-magnetic ion cyclotron (EMIC) waves is included according to quasi-linear theory where the wave amplitudes are provided from statistical models (Shreedevi et al., 2021; Zhu et al. 2021; Tian et al. 2022, Zhu et al., 2022), or the wave growth is calculated selfconsistently with the evolving ring current ion distributions (Jordanova et al., 2001). The wave-induced scattering of relativistic electrons by whistler mode hiss inside the plasmasphere and whistler mode chorus outside the plasmasphere is calculated using either electron lifetimes (Jordanova et al., 2010a), diffusion coefficients from statistical wave models (Yu et al., 2016), or event-specific diffusion coefficients (Jordanova et al., 2016; Yu et al., 2022).

Finally, losses due to field-line curvature scattering induced by nonadiabatic particle motion in weak magnetic fields are incorporated in RAM using either lifetimes (Eshetu et al., 2021) or diffusion coefficients (Yu et al. 2020).

2.2. Self-consistent magnetic field (SCB) model

In order to calculate the magnetic field (**B**) self-consistently with the anisotropic plasma population, RAM was coupled with a 3-D force balance model (e.g., Jordanova et al., 2006, 2010b; ; Zaharia et al., 2006, 2010;) that solves the single-fluid plasma force balance equation:

$$\mathbf{J} \times \mathbf{B} = \nabla \cdot \mathbf{P} = \nabla P_{\perp} - \nabla \cdot \left[(P_{\perp} - P_{\parallel}) \mathbf{b} \mathbf{b} \right] \tag{2}$$

where **J** is the current density, **P** is the pressure tensor, and P_{\perp} and P_{\parallel} are the pressure components perpendicular and parallel to the magnetic field, respectively. This force balance algorithm is valid for the inner magnetosphere, where the flow is subsonic (slow-flow approximation) and the inertia of the plasma can be neglected (Wolf, 1983), and has the capability to compute equilibria where the numerical solution may become MHD unstable. Expressing the magnetic field as $\mathbf{B} = \nabla \alpha_E \times \nabla \beta_E$ in which case a magnetic field line corresponds to the intersection of two (α_E, β_E) Euler potential isosurfaces, the force balance equation can be decomposed into two coupled "quasi 2-D" inhomogeneous partial differential equations:

$$\nabla \cdot \left[(\nabla \alpha_E)^2 \nabla \beta_E - (\nabla \alpha_E \cdot \nabla \beta_E) \nabla \alpha_E \right]$$

$$= -\frac{\mathbf{B} \times \nabla \alpha_E}{\sigma B^2} \cdot \left[\nabla P_\perp + (1 - \sigma) \nabla \left(\frac{B^2}{2} \right) \right]$$
(3)

$$\nabla \cdot \left[(\nabla \beta_E)^2 \nabla \alpha_E - (\nabla \alpha_E \cdot \nabla \beta_E) \nabla \beta_E \right]$$

$$= \frac{\mathbf{B} \times \nabla \beta_E}{\sigma B^2} \cdot \left[\nabla P_{\perp} + (1 - \sigma) \nabla \left(\frac{B^2}{2} \right) \right] \tag{4}$$

Here $\sigma = 1 + (P_{\perp} - P_{\parallel})/B^2$. These equations are solved together with two Maxwell's equations:

$$\nabla \times \mathbf{B} = \mu_{o} \mathbf{J} \tag{5}$$

$$\nabla \cdot \mathbf{B} = 0 \tag{6}$$

The system of equations (3) – (6) is solved numerically using a Picard iteration procedure. The anisotropic plasma pressures in the equatorial plane are supplied from RAM and are mapped along magnetic field lines assuming energy and magnetic moment conservation and an "empty loss cone" formalism (Zaharia et al., 2006).

2.3. Self-consistent magnetic and electric field (SCB-E) model

In addition to including magnetic field self-consistency, the code was further developed to also include a self-consistent electric field coupling with the plasma (Yu et al., 2017). In the case of no parallel potential drop, like

in the inner magnetosphere, the electric field could be derived from the Poisson equation for the electric potential Φ solved at ionospheric altitudes:

$$\nabla \cdot (\Sigma \cdot \nabla \Phi) = -J_{\parallel} \sin I \tag{7}$$

where J_{\parallel} is the density of field-aligned currents (FACs) flowing into and out of the ionosphere, Σ is the height-integrated ionospheric conductance tensor, including both Hall and Pedersen conductances, and I is the magnetic field inclination angle. The FAC density is calculated with a formula obtained considering charge neutrality (Zaharia et al., 2010):

$$\mathbf{B} \cdot \nabla \left(\frac{J_{\parallel}}{B} \right) = \frac{2\mathbf{B} \cdot (\nabla \cdot \mathbf{P} \times \kappa)}{B^2} \tag{8}$$

where $\kappa = (\mathbf{b} \cdot \nabla \mathbf{b})$ is the field line curvature. To obtain FAC density at ionospheric altitudes, Eq. (8) is integrated along magnetic field lines from the equatorial plane to the ionosphere.

Several physical processes contribute to the ionospheric conductance: diffuse auroral precipitation, discrete auroral precipitation, solar EUV radiation, and polar rain. An empirical function (Moen and Brekke, 1993) based on the solar zenith angle and the F10.7 index is used to obtain the dayside conductance associated with solar EUV radiation. A small background conductance is applied over the polar cap above the open/closed field line boundary to include the weak contribution from polar rain. The empirical Robinson relation (Robinson et al., 1987) is employed to calculate the diffusive aurora conductance using the precipitation energy flux obtained from RAM, as well as the discrete aurora conductance using the FACs calculations described above. The auroral conductance can also be determined in a more physics-based manner by passing RAM's particle precipitating flux to a 3-D ionospheric electron transport code. Further details on the calculation of the electron precipitation from RAM and its mapping to ionospheric altitudes to calculate the auroral conductance are provided in Yu et al. (2016, 2017). The coupling of RAM-SCB-E with the ionospheric electron transport model GLOW (GLobal airglOW) that performs the calculation of the auroral conductance from first principles (i.e., including the atmospheric ionization and emission created by electron precipitation) is described in Yu et al. (2018). In this case, the GLOW model takes RAM's electron precipitating flux as input and computes vertical profiles of Hall and Pedersen conductivities; these profiles are then integrated over altitude to yield the conductance. The version of the code with self-consistent electric field (RAM-SCB-E) is still under active development.

2.4. Data assimilation framework

An ensemble-based data assimilation framework has been developed to improve RAM-SCB nowcast and potential forecast when in situ measurements are available. The method applied to RAM-SCB is an Ensemble Kalman Fil-

ter (EnKF) with orthonormal projections and is described in Godinez et al. (2016). This approach was applied to simulate the enhancement of the ring current during geomagnetically active periods of time. The state of the ring current was corrected using proton flux observations from the Magnetic Electron and Ion Spectrometer (MagEIS) instrument on both Van Allen Probes A and B to better calibrate the model solution. Fig. 2a and 2b show the particle pressure in the equatorial plane for a model simulation without data assimilation (left plot in each panel) and with data assimilation (right plot in each panel) for (a) 12:00 UTC and (b) 14:00 UTC. In order to assess the forecast error, we performed a validation experiment, where we assimilated the proton flux only from Van Allen Probe A and compared the assimilated result against Van Allen Probe B. The normalized root mean square (RMS) error in the spin-averaged flux for energies below 200 keV from this validation experiment is shown along the Van Allen Probe B orbit in Fig. 2c. It is evident that this approach could provide orders of magnitude improvement in model fluxes and is a promising tool to better characterize the surface charging environment. It should be noted, however, that RAM-SCB with data assimilation requires significantly more computational resources than without, as the assimilation process requires an ensemble of RAM-SCB simulation to be run simultaneously to create the necessary input for the EnKF algorithm.

3. Required inputs, installation and execution

In RAM-SCB the kinetic equation (1) is written in conservative form (Jordanova et al., 1996) which preserves the total number of particles and is thus better for numerical implementation. For input, RAM requires an initial distribution function, an outer boundary flux, as well as prescribed electric and magnetic fields. The SCB code requires as inputs plasma pressure and an outer magnetic field boundary. Recent updates to the numerical implementation of the equations and the coupling between the two models with the goal of improving the robustness of RAM-SCB are described in Engel et al. (2019).

3.1. Numerical grid, initial and boundary conditions

The RAM domain is a circle in the magnetic equatorial plane, extending from 2 $R_{\rm E}$ out to 6.5 $R_{\rm E}$ by default, with a grid resolution of 0.25 $R_{\rm E}$ and 0.5 MLT. Usually, the resolution is kept fixed for the entire simulation, although RAM has been updated to include the infrastructure for adaptive grid resolution. In addition, the code has the capability to output initialization files at any desired time during a simulation, making it easy to split and restart a simulation. The initial conditions could be set up after satellite observations or by using a restart file from a previous simulation. Typically, the model is run for \sim 6 h of quiet time before the storm commencement to obtain a realistic initialization.

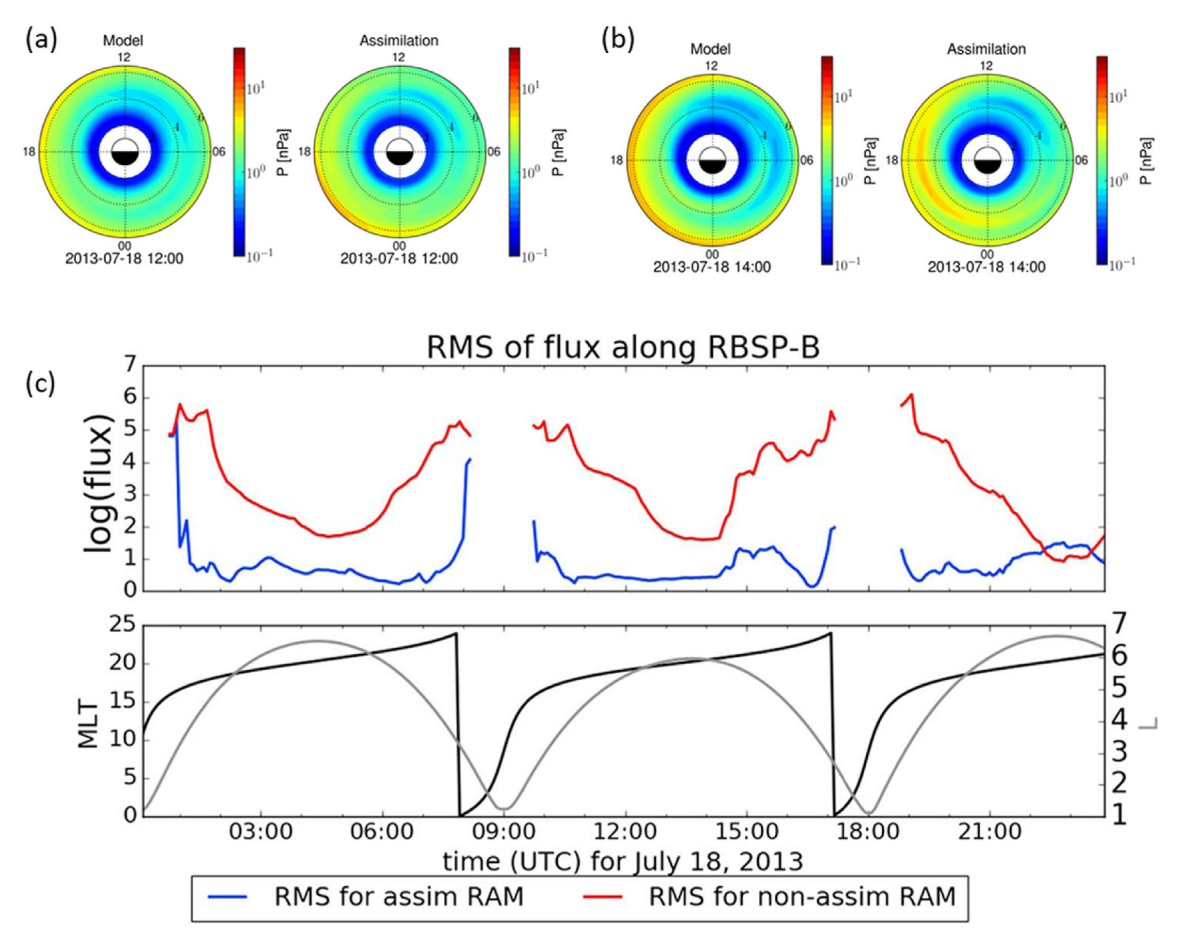


Fig. 2. (top) Ring current pressure at the geomagnetic equator at (a) 12:00 UT and (b) 14:00 UT from (left column) unassimilated model result and (right column) assimilated model result with data from the Van Allen Probes A and B flying near the equator during 18 July 2013. (bottom) Root mean square (RMS) error of the flux along the Van Allen Probe B trajectory for a validation experiment (assimilating proton flux from Van Allen Probe A and comparing the assimilated result against Probe B).

The RAM flux boundary conditions determine the particles that enter the simulation from the outer edge and are typically derived from LANL GEO satellite measurements or Kp-driven analytical models. RAM is capable of running with an analytic magnetic field model, but the inclusion of the self-consistent magnetic field component (SCB) provides a much better result. SCB requires the specification of an outer boundary in order to solve the forcebalanced equations, which can be provided through the various Tsyganenko magnetic field models as well as event fitted models (e.g., Brito and Morley, 2017). Like the magnetic field, the electric field can be provided using a number of different models as mentioned above; by default, the Volland-Stern electric potential is calculated using the Kp index. Additionally, if solar wind data is provided to RAM, the Weimer electric potential models can be used to calculate the electric field. The Weimer model also acts as the boundary condition for the self-consistent electric field.

In addition, RAM-SCB may be used as a component of the Space Weather Modelling Framework (SWMF) (e.g., Welling et al., 2018). Under this mode, RAM-SCB receives initial and boundary conditions from the Framework's other components and returns plasma properties to create a two-way coupled system.

3.2. Installation and performing simulations

RAM-SCB is developed and tested on the linux operating system, and while installation and simulation may be possible on other systems, this is not currently supported. To install RAM-SCB the system must satisfy the prerequisites. That is, the GNU Scientific Library (GSL) must be present, and NetCDF-Fortran must be installed. As the build system leverages the SWMF build system, Perl is also required. Once the prerequisites have been installed, the user can configure the build and compile the code. Under the SWMF build system compilers are required that support Fortran, C and C++. RAM-SCB is developed and tested with gfortran, gcc and g++. Build configuration sets up the make system and tells RAM-SCB where to find its dependencies. RAM-SCB supports auto-detecting the locations of NetCDF and GSL, assuming that the command line utilities are properly installed.

The standard usage of RAM-SCB mirrors that of SWMF, such that the code builds in place, and is not strictly installed. For simulations, a run directory must first be generated, and this can be performed using the build system. The default run directory provides a configuration file along with initial and boundary conditions for some test simulations. The user is directed to RAM-SCB's documentation for setting up simulations.

4. Example applications

The RAM model has been used extensively over the past > 25 years to study various aspects of inner magnetosphere dynamics. At first, it was employed to simulate the effects of transport, energization, and loss in a dipolar model of the Earth's magnetic field on the major ring current ion species, i.e., H⁺, O⁺, and He⁺ (e.g., Jordanova et al., 1996, 2001; Kozyra et al., 2002; Liemohn et al., 2000) as well as on the relativistic electrons (Jordanova et al., 2008; 2010a). Later, RAM was extended to non-dipolar magnetic field geometry and coupled with SCB to study these effects in a self-consistently calculated magnetic field (e.g., Jordanova et al., 2006; 2010b; Zaharia et al., 2006; 2010). Several representative examples from recent RAM-SCB studies that demonstrate its space weather applicability are provided in this section.

4.1. Stand-alone RAM-SCB

The RAM-SCB code has been improved significantly during the SHIELDS project (Jordanova et al., 2018) in order to simulate accurately the surface charging electron environment during periods of intense geomagnetic activity. Not only the models have been modernized and made more user friendly, but also a number of changes to their functionality like decoupling of the RAM and SCB grids, improvements to the force balancing methods, and proper tracking of the magnetopause have been implemented (Engel et al., 2019). These new capabilities were demonstrated with a simulation of the 17 March 2013 geomagnetic storm, where the integrated > 10 keV electron flux was used as one of the metrics (Fig. 3a); elevated fluxes at these energies can imply a satellite surface charging hazard. Results from the new model (blue line) showed much better agreement with Van Allen Probe observations (black line) than results from the old model (red line). As shown by Engel et al. (2019), the new model configuration reproduced better the observed sym-H index too (Fig. 3b) and reduced its RMS error by more than a factor of 2, demonstrating a significant quantitative improvement in the simulation.

Recently, we used RAM-SCB to investigate ring current variations during the 7–8 November 2017 geomagnetic storm and showed that the ion and electron fluxes measured by the Arase satellite were fairly well reproduced (Kumar et al., 2021). To study the spatial/longitudinal variation in the ring current we used observations from

30 low to midlatitude (09°–45° MLat) ground magnetic stations, which showed clear dawn-dusk asymmetry during this storm period. We compared the contribution of the different charged particle species (H⁺, He⁺ and O⁺ ions and electrons) to the horizontal magnetic field deformation (Δ H) observed at these ground magnetic stations. In general, RAM-SCB results showed that the electrons contributed ~12 % to the total ring current pressure while the ions contributed ~88 % and were the major contributor. However, during the main phase of the storm the electron contribution was non-negligible (~18 %) in the dawn-side, and thus ring current electrons have contributed significantly to the negative Δ H variations observed at ground in the dawn sector.

4.2. RAM-SCB coupled with SWMF

Besides the capability to run RAM-SCB as a standalone model, it can also be used as a flexible tool that is fully coupled to the Space Weather Modeling Framework (SWMF) (e.g., Welling et al., 2018; Yu et al., 2014, 2016; Zaharia et al., 2010). This option allows the user to explore how the ring current interacts with the magnetosphere-iono sphere-thermosphere system. The SWMF handles the coupling between RAM-SCB as an inner magnetosphere component with BATSRUS (the global magnetosphere component) and RIM (the ionospheric electrodynamics component). In this case, RAM-SCB uses input from BATSRUS to specify the plasma and magnetic field boundary conditions at GEO, and the RIM ionospheric electric potential mapped along SCB magnetic field lines to the equatorial plane to calculate particle drifts. In return, RAM-SCB passes the total plasma pressure to BATSRUS to correct the MHD solution, and electron precipitation to RIM to update the ionospheric conductance. The coupling between the models allows for the development of feedback loops and various consequences, such as increased pressure in the inner magnetosphere and stretching of the MHD magnetotail. As a result, more realistic values of the Dst index are obtained (Welling et al., 2018).

Several versions of these models were used in the community-wide challenge organized by the Geospace Environment Modeling (GEM) program to assess the capability of inner magnetosphere models in determining the surface charging environment for the Van Allen Probes during a geomagnetic storm event (Yu et al., 2019). For this challenge, the storm of 17 March 2013 was selected as one of the major storms that has been extensively studied by the community. Fig. 4 demonstrates the results from this GEM challenge, where the observed electron flux (black line) integrated between 10 and 50 keV was used as the metrics and was compared with four different simulations (color lines). In addition, to quantitatively measure the model performance against observations, several skill scores (e.g., prediction efficiency, cross correlation, rootmean-square error, prediction yield, and symmetric signed

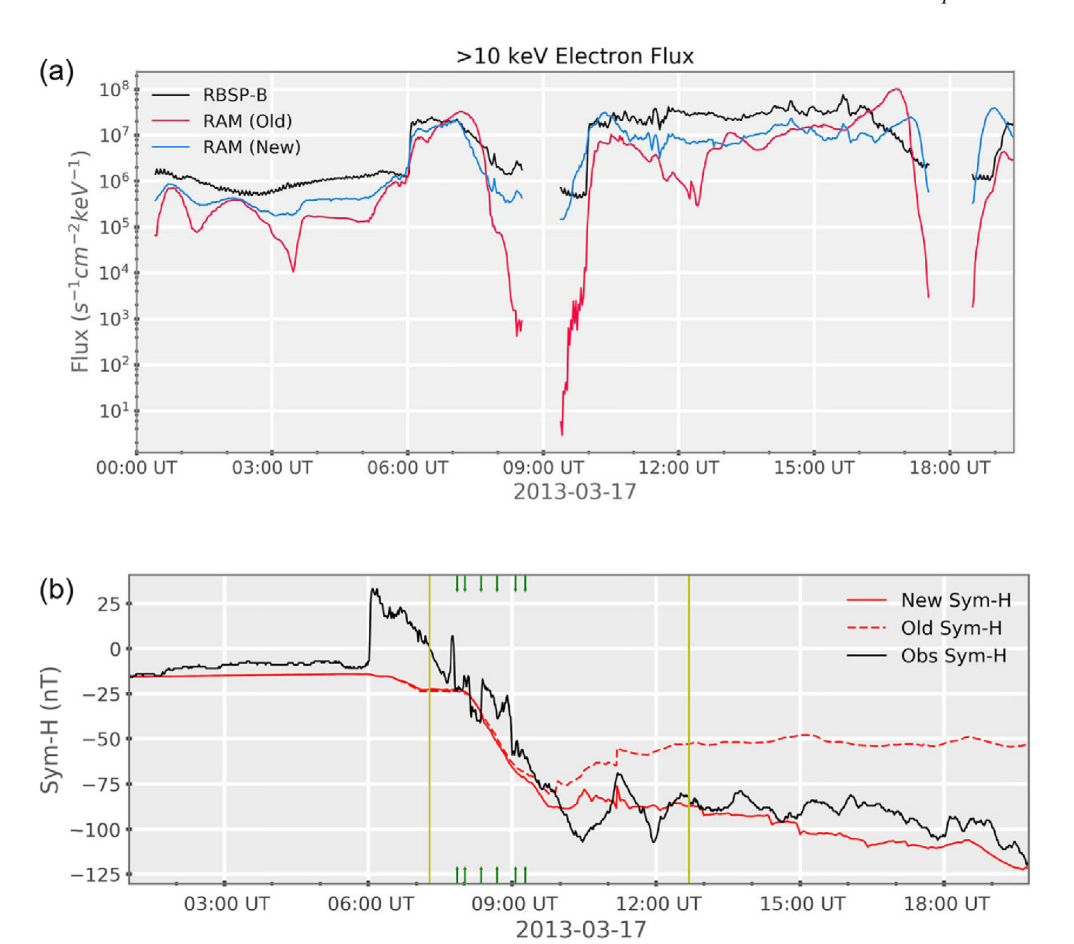


Fig. 3. (a) The integrated > 10 keV electron flux from RBSP-B HOPE and MagEIS instruments (black line), the new model (blue line) and the old model (red line). The fluxes are masked over the time periods where RBSP-B was outside the RAM domain. (b) The observed *sym*-H (solid black line) compared with the calculated *sym*-H for the new model (red solid line) and the old model (red dashed line) configurations. *Source: From* Engel et al. (2019).

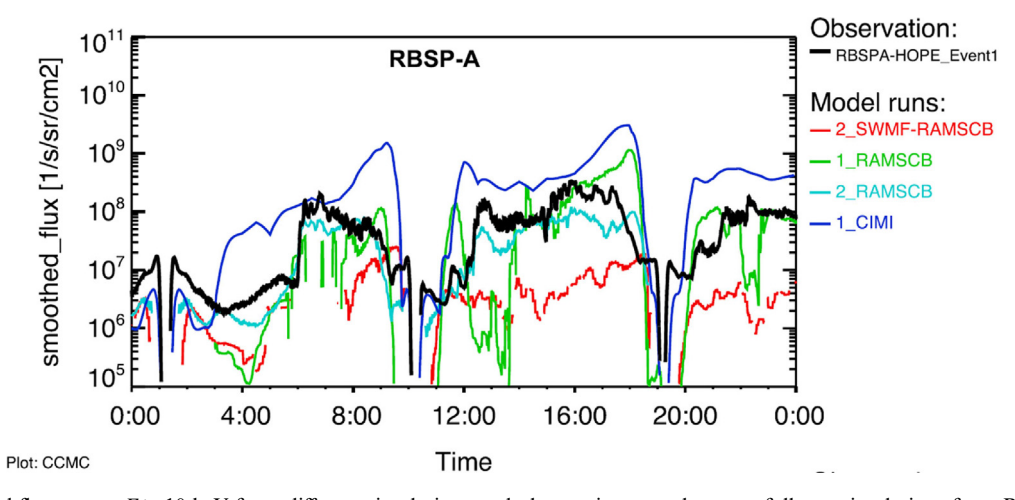


Fig. 4. The integrated fluxes over E > 10 keV from different simulations and observations are shown as follows: simulations from RAM-SCB driven by Volland-Stern electric field (green), RAM-SCB driven by Weimer electric field (light blue), and RAM-SCB driven by SWMF (red); Comprehensive Inner Magnetosphere-Ionosphere (CIMI) simulations (blue); RBSP observations from the Van Allen Probes A - Helium, Oxygen, Proton, and Electron (HOPE) instrument (black). *Source: From* Yu et al. (2019).

percentage bias) were applied. Although no model excelled in all skill scores, it was found that RAM-SCB driven by observational boundary conditions at GEO generally reproduced the most realistic flux. The electric field also played a crucial role in effectively transporting the plasma toward the Earth, highlighting the importance of its realistic representation.

4.3. Near real-time version

During the SHIELDS project (Jordanova et al., 2018) we started developing a near real-time version of RAM-SCB with the key aim of predicting energy spectra of particle fluxes along specified satellite trajectories. For longterm simulations with operational implications, we require that the simulation configuration be robust, and that the simulation will run faster than real time with limited resources. To this end, our initial near real-time version uses a centered dipole magnetic field model. For specification of the flux outer boundary, we need to ensure that data are available, and to ensure that both nowcasts and forecasts can be made we use models of fluxes at GEO (Denton et al., 2015, 2016). When driven by a prediction of the Kp index this allows several hours of lead time, and when using upstream solar wind data as a driver the lead time is reduced to less than an hour. An example output using forecasted Kp to drive the model and providing a 3-hour prediction of the electron flux (1–400 keV) along Van Allen Probe A trajectory is shown in Fig. 5.

Depending on available resources, more complex configurations may be appropriate for nowcasting and forecasting use, including substituting the centered dipole magnetic field with the self-consistent model using a more realistic outer magnetic field boundary (e.g., Tsyganenko, 1989) that can also be used in a predictive mode. Following the recent updates to the numerical implementation of RAM-SCB described in section 3.1 (cf. Engel et al., 2019) we anticipate that configurations appropriate to near-real time or predictive use will be robust enough to consider for operations. These candidate configurations will be tested for robustness as part of our forthcoming transition towards providing RAM-SCB as an on-demand service (see section 5).

5. Future directions

Accurate modeling of the near-Earth space environment has important scientific and societal implications. This paper highlights current RAM-SCB capabilities and recent improvements to simulate inner magnetosphere dynamics. We envision several possibilities for future RAM-SCB model development and its space weather applications, which are the following:

1. Building on the recent improvements in robustness, and the real time demonstration described in section 4.3, we are now working, in partnership with NASA's Community Coordinated Modeling Center (CCMC), towards providing RAM-SCB as an on-request service. This work will include ensuring that RAM-SCB can use CCMC data sources to specify the necessary inputs and boundary conditions. By starting with simpler configurations, such as the real time configuration, we can ensure that the workflow from user request to quicklook visualization is robust before enabling greater flexibility

- for users of CCMC's runs on request. Making RAM-SCB more accessible via CCMC also requires expansion of the documentation to include guidelines for use, and development of streamlined tools to calculate and visualize derived products.
- 2. An International Space Weather Action Team (ISWAT) on the near-Earth radiation and plasma environment (G3) was recently formed to enhance collaborations among scientists worldwide with the goal to advance understanding of this environment and its potential harmful effects on spacecraft electronics or life in space. Modeling capabilities were recognized as important tools for near real-time monitoring and forecasting of this space plasma environment. As a first step, several benchmarking challenges were organized to assess the performance of models that use GEO measurements for the outer boundary condition. We are taking active participation in the surface charging benchmarking challenge organized by ISWAT G3-02 and are performing simulations with RAM-SCB for the selected challenge events; these results will be delivered to CCMC for further analysis.
- 3. The data assimilation method in RAM-SCB has been able to provide an improved forecast compared to a simulation without data assimilation. The current implementation uses a simplified dipole magnetic field. The near-future plan is to test the data assimilation with a more realistic magnetic field. Additionally, there is data available on other particle species, which will be used to further improve the RAM-SCB forecast by assimilating multiple particle species into the model. Finally, the implementation of machine learning techniques into RAM-SCB is being considered, specifically for the estimation of a self-consistent magnetic field computation. Using machine learning to provide an estimate of the magnetic field will improve computational costs and simulation time, which can be used to speed-up the data assimilation.
- 4. Finally, as a component of the SWMF, the RAM-SCB code will help improve the physics-based modeling of geomagnetic disturbances and GICs. These disturbances depend strongly on the field-aligned current closure through the ionosphere and thus on the ionospheric conductance. We are implementing the addition of electron and ion precipitation from RAM-SCB into the calculation of the ionospheric conductance. This approach will provide much better, dynamic specification of the ionospheric conductance compared to statistical models. This improvement is especially needed during highly disturbed periods when GIC effects become significant and will be the subject of future studies.

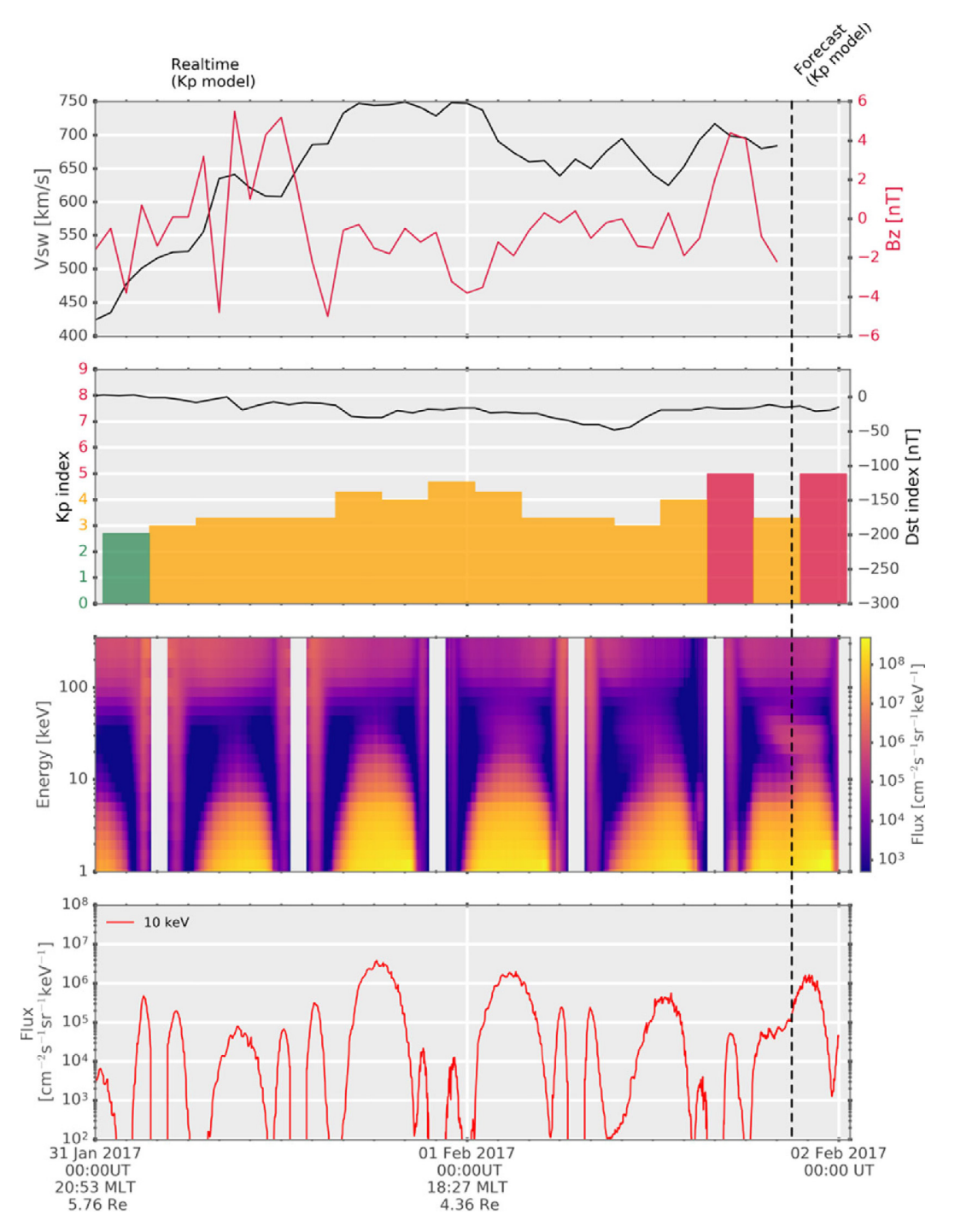


Fig. 5. Output of the near real-time model showing a 3-hour prediction along Van Allen Probe A satellite trajectory during 01 February 2017. From top to bottom the panels show solar wind velocity and IMF Bz, the Kp and Dst indices, simulated electron flux spectrogram, and 10-keV electron flux. *Source: From Jordanova* et al. (2018).

Declaration of Competing Interest

The authors declare that they have no known competing financial interests or personal relationships that could have appeared to influence the work reported in this paper.

Acknowledgments

Work at Los Alamos was performed under the auspices of the U.S. Department of Energy (Contract No. 89233218CNA000001) and was partially funded by NASA grants 80HQTR19T0058 and 80HQTR21T0008 and NSF grant IAA2027951. Work at Beihang University was supported by the National Natural Science Foundation of

China (NSFC) grants 41974192 and 41821003. RAM-SCB is an open-source software that can be downloaded from GitHub (https://github.com/lanl/RAM-SCB).

References

- Brito, T.V., Morley, S.K., 2017. Improving empirical magnetic field models by fitting to in situ data using an optimized parameter approach. Space Weather. 15, 1628–1648. https://doi.org/10.1002/ 2017SW001702.
- Denton, M.H., Thomsen, M.F., Jordanova, V.K., Henderson, M.G., Borovsky, J.E., Denton, J.S., Pitchford, D., Hartley, D.P., 2015. An empirical model of electron and ion fluxes derived from observations at geosynchronous orbit. Space Weather. 13, 233–249. https://doi.org/ 10.1002/2015SW001168.
- Denton, M.H., Henderson, M.G., Jordanova, V.K., Thomsen, M.F., Borovsky, J.E., Woodroffe, J., Hartley, D.P., Pitchford, D., 2016. An improved empirical model of electron and ion fluxes at geosynchronous orbit based on upstream solar wind conditions. Space Weather. 14, 511–523. https://doi.org/10.1002/2016SW001409.
- Engel, M.A., Morley, S.K., Henderson, M.G., Jordanova, V.K., Woodroffe, J.R., Mahfuz, R., 2019. Improved simulations of the inner magnetosphere during high geomagnetic activity with the RAM-SCB model. J. Geophys. Res.: Space Phys. 124, 4233–4248. https://doi.org/ 10.1029/2018JA026260.
- Eshetu, W.W., Tu, W, Jordanova, V.K., Cowee, M., 2021. Quantifying the effect of magnetic field line curvature scattering on the loss of ring current ions. J. Geophys. Res.: Space Phys. 126, 1–18. https://doi.org/10.1029/2020JA028497.
- Godinez, H.C., Yu, Y., Lawrence, E., Henderson, M.G., Larsen, B., Jordanova, V.K., 2016. Ring current pressure estimation with RAM-SCB using data assimilation and Van Allen Probe flux data. Geophys. Res. Lett. 43, 11948–11956. https://doi.org/10.1002/2016GL071646.
- Gubby, R., Evans, J., 2002. Space environment effects and satellite design. J. Atmos. Sol. Terr. Phys. 64 (16), 1723–1733. https://doi.org/10.1016/ S1364-6826(02)00122-0.
- Jordanova, V.K., Kistler, L.M., Kozyra, J.U., Khazanov, G.V., Nagy, A. F., 1996. Collisional losses of ring current ions. J. Geophys. Res.: Space Phys. 101 (A1), 111–126. https://doi.org/10.1029/95JA02000.
- Jordanova, V.K., Kozyra, J.U., Nagy, A.F., Khazanov, G.V., 1997. Kinetic model of the ring current-atmosphere interactions. J. Geophys. Res.: Space Phys. 102 (A7), 14279–14291. https://doi.org/10.1029/96JA03699.
- Jordanova, V.K., Farrugia, C.J., Thorne, R.M., Khazanov, G.V., Reeves, G.D., Thomsen, M.F., 2001. Modeling ring current proton precipitation by electromagnetic ion cyclotron waves during the May 14–16, 1997, storm. J. Geophys. Res. 106 (A1), 7–22. https://doi.org/10.1029/2000JA002008.
- Jordanova, V.K., Miyoshi, Y.S., Zaharia, S., Thomsen, M.F., Reeves, G. D., Evans, D.S., et al., 2006. Kinetic simulations of ring current evolution during the Geospace Environment Modeling challenge events. J. Geophys. Res. 111(A11), A11S10, 1–16. https://doi.org/10.1029/2006JA011644.
- Jordanova, V.K., Albert, J., Miyoshi, Y., 2008. Relativistic electron precipitation by EMIC waves from self-consistent global simulations. J. Geophys. Res.: Space Phys. 113(A3), A00A10, 1–11. https://doi.org/ 10.1029/2008JA013239.
- Jordanova, V.K., Thorne, R.M., Li, W., Miyoshi, Y., 2010a. Excitation of whistler mode chorus from global ring current simulations. J. Geophys. Res. 115, A00F10, 1–12. https://doi.org/10.1029/ 2009JA014810.
- Jordanova, V.K., Zaharia, S., Welling, D.T., 2010b. Comparative study of ring current development using empirical, dipolar, and self-consistent magnetic field simulations. J. Geophys. Res.: Space Phys. 115, A00J11, 1–17. https://doi.org/10.1029/2010JA015671.
- Jordanova, V.K., Tu, W., Chen, Y., Morley, S.K., Panaitescu, A.D., Reeves, G.D., Kletzing, C.A., 2016. RAM-SCB simulations of electron

- transport and plasma wave scattering during the October 2012 "double-dip" storm. J. Geophys. Res.: Space Phys. 121, 8712–8727. https://doi.org/10.1002/2016JA022470.
- Jordanova, V.K., Delzanno, G.L., Henderson, M.G., Godinez, H.C., Jeffery, C.A., et al., 2018. Specification of the near-Earth space environment with SHIELDS. J. Atm. Sol. Terr. Phys. 177, 148–159. https://doi.org/10.1016/j.jastp.2017.11.006.
- Kozyra, J.U., Liemohn, M.W., Clauer, C.R., Ridley, A.J., Thomsen, M. F., Borovsky, J.E., Roeder, J.L., Jordanova, V.K., 2002. Two-step Dst development and ring current composition changes during the 4–6 June 1991 magnetic storm. J. Geophys. Res. 107 (A8), 1–22. https://doi.org/10.1029/2001JA000023.
- Kumar, S., Miyoshi, Y., Jordanova, V.K., Engel, M., Asamura, K., Yokota, S., et al., 2021. Contribution of electron pressure to ring current and ground magnetic depression using RAM-SCB simulations and Arase observations during 7–8 November 2017 magnetic storm e2021JA029109. J. Geophys. Res.: Space Phys. 126, 1–16. https://doi.org/10.1029/2021JA029109.
- Liemohn, M.W., Kozyra, J.U., Richards, P.G., Khazanov, G.V., Buonsanto, M.J., Jordanova, V.K., 2000. Ring current heating of the thermal electrons at solar maximum. J. Geophys. Res. 105, 27767–27776. https://doi.org/10.1029/2000JA000088.
- Mate, A., Barnes, A.K., Morley, S.K., Friz-Trillo, J.A., Cotilla-Sanchez, E., Blake, S.P., 2021. Relaxation Based Modeling of GMD Induced Cascading Failures in PowerModelsGMD.jl, 2021 North American Power Symposium NAPS, 1–7. https://doi.org/10.1109/NAPS52732.2021.9654450.
- Moen, J., Brekke, A., 1993. The solar flux influence on quiet time conductances in the auroral ionosphere. Geophys. Res. Lett. 20, 971– 974. https://doi.org/10.1029/92GL02109.
- Morley, S.K., 2020. Challenges and opportunities in magnetospheric space weather prediction e2018SW002108. Space Weather. 18, 1–22. https://doi.org/10.1029/2018SW002108.
- Rairden, R.L., Frank, L.A., Craven, J.D., 1986. Geocoronal imaging with Dynamics Explorer. J. Geophys. Res. 91, 13613–13630. https://doi. org/10.1029/JA091iA12p13613.
- Rasmussen, C.E., Guiter, S.M., Thomas, S.G., 1993. A two-dimensional model of the plasmasphere: Refilling time constants. Planet. Space Sci. 41 (1), 35–43. https://doi.org/10.1016/0032-0633(93)90015-T.
- Robinson, R.M., Vondrak, R.R., Miller, K., Dabbs, T., Hardy, D., 1987.
 On calculating ionospheric conductances from the flux and energy of precipitating electrons. J. Geophys. Res. 92, 2565–2569. https://doi.org/10.1029/JA092iA03p02565.
- Shreedevi, P.R., Yu, Y., Ni, B., Saikin, A., Jordanova, V.K., 2021. Simulating the ion precipitation from the inner magnetosphere by H-band and He-band electro magnetic ion cyclotron waves e2020JA028553. J. Geophys. Res.: Space Phys. 126, 1–21. https://doi.org/10.1029/2020JA028553.
- Stern, D.P., 1975. The motion of a proton in the equatorial magneto-sphere. J. Geophys. Res.: Space Phys. 80 (4), 595–599. https://doi.org/10.1029/JA080i004p00595.
- Tian, X., Yu, Y., Zhu, M., Cao, J., Shreedevi, P.R., Jordanova, V.K., 2022. Effects of EMIC wave-driven ion precipitation on the ionosphere e2021JA030101. J. Geophys. Res.: Space Phys. 127, 1–15. https://doi. org/10.1029/2021JA030101.
- Tsyganenko, N.A., 1989. A magnetospheric magnetic field model with a warped tail current sheet. Planet. Space Sci. 37 (1), 5–20. https://doi.org/10.1016/0032-0633(89)90066-4.
- Tsyganenko, N.A., 1996. Effects of the solar wind conditions on the global magnetospheric configuration as deduced from data-based field models. Eur. Space Agency Spec. Publ. ESA SP. 389, 181–185.
- Tsyganenko, N.A., Sitnov, M.I., 2005. Modeling the dynamics of the inner magnetosphere during strong geomagnetic storms. J. Geophys. Res. 110 (A03208), 1–16. https://doi.org/10.1029/2004JA010798.
- Volland, H., 1973. A semiempirical model of large-scale magnetospheric electric fields. J. Geophys. Res. 78 (1), 171–180. https://doi.org/ 10.1029/JA078i001p00171.

- Weimer, D.R., 2001. Maps of ionospheric field-aligned currents as a function of the interplanetary magnetic field derived from Dynamics Explorer 2 data. J. Geophys. Res.: Space Phys. 106 (A7), 12889–12902. https://doi.org/10.1029/2000JA000295.
- Weimer, D.R., 2005. Improved ionospheric electrodynamic models and application to calculating Joule heating rates. J. Geophys. Res. 110 (A05306), 1–21. https://doi.org/10.1029/2004JA010884.
- Welling, D.T., Toth, G., Jordanova, V.K., Yu, Y., 2018. Integration of RAM-SCB into the Space Weather Modeling Framework. J. Atmos. Sol. Terr. Phys. 177, 160–168. https://doi.org/10.1016/j.jastp.2018.01.007.
- Wolf, R., 1983. The quasi-static (slow-flow) region of the magnetosphere. In: Solar-terrestrial physics. Springer, Berlin, pp. 303–368.
- Yu, Y., Tian, X., Jordanova, V.K., 2020. The effects of field line curvature (FLC) scattering on ring current dynamics and isotropic boundary e2020JA027830. J. Geophys. Res.: Space Phys. 125, 1–17. https://doi.org/10.1029/2020JA027830.
- Yu, Y., Hosokawa, K., Ni, B., Jordanova, V.K., Miyoshi, Y., Cao, J., et al., 2022. On the importance of using event-specific wave diffusion rates in modeling diffuse electron precipitation e2021JA029918. J. Geophys. Res.: Space Phys. 127. https://doi.org/10.1029/2021JA029918.
- Yu, Y., Jordanova, V., Welling, D., Larsen, B., Claudepierre, S.G., Keltzing, C., 2014. The role of ring current particle injections: Global simulations and Van Allen Probes observations during 17 March 2013 storm. Geophys. Res. Lett. 41, 1126–1132. https://doi.org/10.1002/ 2014GL059322.
- Yu, Y., Jordanova, V.K., Ridley, A.J., Albert, J.M., Horne, R.B., Jeffery, C.A., 2016. A new ionospheric electron precipitation module coupled with RAM-SCB within the geospace general circulation model. J. Geophys. Res.: Space Phys. 121 (9), 8554–8575. https://doi.org/10.1002/2016JA022585.

- Yu, Y., Jordanova, V.K., Ridley, A.J., Toth, G., Heelis, R., 2017. Effects of electric field methods on modeling the midlatitude ionospheric electrodynamics and inner magnetosphere dynamics. J. Geophys. Res.: Space Phys. 122 (5), 5321–5338. https://doi.org/10.1002/ 2016JA023850.
- Yu, Y., Jordanova, V.K., McGranaghan, M., Solomon, S., 2018. Self-consistent modeling of electron precipitation and response in the ionosphere: application to low-altitude energization during substorms. Geophys. Res. Lett. 45 (13), 6371–6381. https://doi.org/10.1029/2018GL078828
- Yu, Y., Rastätter, L., Jordanova, V.K., Zheng, Y., Engel, M., Fok, M.-C., Kuznetsova, M.M., 2019. Initial results from the GEM challenge on the spacecraft surface charging environment. Space Weather. 17, 299– 312. https://doi.org/10.1029/2018SW002031.
- Zaharia, S., Jordanova, V.K., Thomsen, M.F., Reeves, G.D., 2006. Self-consistent modeling of magnetic fields and plasmas in the inner magnetosphere: Application to a geomagnetic storm. J. Geophys. Res.: Space Phys. 111, A11S14, 1–14. https://doi.org/10.1029/2006JA011619.
- Zaharia, S., Jordanova, V.K., Welling, D.T., Toth, G., 2010. Self-consistent inner magnetosphere simulation driven by a global MHD model. J. Geophys. Res.: Space Phys. 115, A12228, 1–21. https://doi.org/10.1029/2010JA015915.
- Zhu, M., Yu, Y., Tian, X., Shreedevi, P.R., Jordanova, V.K., 2021. On the ion precipitation due to field line curvature (FLC) and EMIC wave scattering and their subsequent impact on ionospheric electrodynamics e2020JA028812. J. Geophys. Res.: Space Phys. 126, 1–17. https://doi. org/10.1029/2020JA028812.
- Zhu, M., Yu, Y., Cao, X., Ni, B.B., Tian, X.B., Cao, J.B., Jordanova, V. K., 2022. Effects of polarization-reversed EMIC waves on the ring current dynamics. Earth Planet Phys. 6, 329–338. https://doi.org/10.26464/epp2022037.